WELDING RESEARCH

SUPPLEMENT TO THE *WELDING JOURNAL*, JANUARY 1999
Sponsored by the American Welding Society and the Welding Research Council

Transient Thermal Analysis of Spot Welding Electrodes

A parametric model was developed to predict thermal behavior of electrode cap

BY K. S. YEUNG AND P. H. THORNTON

ABSTRACT. The accurate thermal simulation of a spot welding electrode cap could permit critical design parameters to be identified for improved electrode life. In this study, a parametric model has been developed to predict the transient thermal behavior of a typical spot welding electrode cap. The model employs the technique of conjugate heat transfer analysis to avoid the problem of estimating a value for the heat transfer coefficient that arises with conventional heat transfer analysis.

Using experimental values for the input power, the predicted maximum tip surface temperature was 905 K. Traces of aluminum melting at the cap/aluminum interface are often observed in practice in the spot welding of aluminum. Since aluminum alloys have melting points of ~900 K, the simulation closely predicts the tip surface temperature.

The analysis indicated that convective and radiant heat losses were not important. A simple linear relationship between the maximum temperature and the input power was found. For very short heating times, no significant changes were found in the maximum temperature reached for a decrease of the coolant flow rate from 3.79 L/min (1.00 gal/min) to 2.24 L/min (0.75 gal/min), or for a decrease of the cap depth — the distance between the tip working surface and the cooling surface — from 9.00–6.35 mm. The overall behavior is typical to that of components with a slow thermal response, but a fast heating rate.

Introduction

Electric resistance spot welding has been used for many years in the automotive industry for joining body sheet components, and it is particularly well-suited for uncoated, low carbon steel. The effectiveness of the process depends, to a considerable extent, on electrode cap life. Coatings on the steel and other metals (*e.g.*, aluminum) can reduce electrode life. Many factors — thermal, electrical, mechanical and metallurgical — influence electrode cap life.

Electrode caps are subject to severe thermal operating conditions and mechanical forces that are responsible for electrode deterioration (*e.g.*, wear, tip contamination, tip mushrooming), which leads to a decline in weld quality and a reduced electrode life. The degradation is particularly acute in spot welding galvanized steel and aluminum alloys, and the correction of such problems during production often necessitates on-line maintenance.

In the spot welding process, thermal conditions at the two main interfaces — the faying surface, which is the workpiece/workpiece interface, and the electrode/workpiece interface — are particularly critical. The faying surface temperature affects the size and quality of the welds. Since excessive heating at the electrode/workpiece surface gives rise to cap deterioration, for a long electrode life the temperature should be kept as low as possible, while maintaining a higher temperature at the workpiece faying surfaces.

Knowledge of temperature distribution in the electrode cap could be of importance to improved electrode life and for the maintenance of spot weld quality, *e.g.*, by suggesting changes in the electrode design. Temperatures adjacent to the tip surface have been measured (Refs. 1, 2), but because of experimental limitations associated with the physical size of the thermocouples used in the determinations, the temperature values measured were not those exactly on the surface. Since the thermal gradients near the surface are very large (Ref. 1), the surface temperatures can be determined only by extrapolation.

Numerical methods (Refs. 3–5) have been employed to predict cap temperature distributions. However, these models did not consider the presence of water in the cooling chamber of the tip, and the heat loss of the electrode to the coolant either was estimated or determined experimentally. The object of this investigation was to determine the temperature distribution (in particular, the maximum tip surface temperature) without relying upon heat loss test data.

In heat transfer analysis, the energy equation must be coupled with the equations of continuity and motion to describe the process of heat conduction and convection. In classical heat transfer analysis, convection has been considered only as one type of thermal boundary condition to be applied at the surface of a conducting solid. This amounts to decoupling the energy equation from those of continuity and motion. In this approach, since convection is given at the boundary, only the energy equation is required. However, values for the convection coefficients required can vary by

K. S. YEUNG and P. H. THORNTON are with Scientific Research Laboratories, Ford Motor Company, Dearborn, Mich.

KEY WORDS

Resistance Spot Welding Electrodes
Electrode Cap
Transient Thermal Analysis
Parametric Model
Aluminum
Conjugate Heat Transfer Analysis

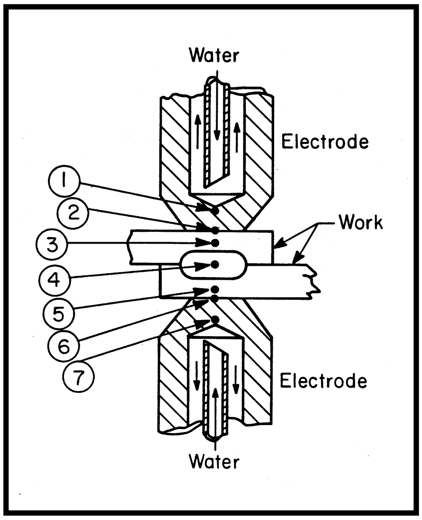

Fig. 1 — Electric resistance spot welding.

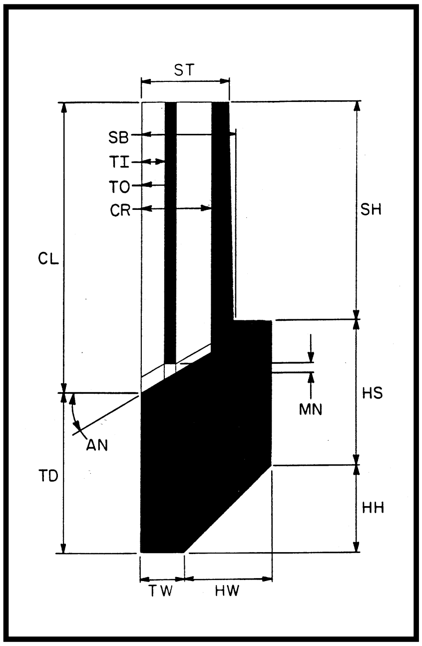

Fig. 2 — Electrode geometry.

two orders of magnitude and are very difficult to estimate, particularly for real world situations (Ref. 6).

An alternative approach, as described in this paper, is conjugate heat transfer analysis, using computational fluid dynamics software (Refs. 7, 8). In this method, the highly nonlinear coupled governing equations of continuity, motion and energy in fluid mechanics and heat transfer are solved, thus permitting the simultaneous determination of the temperature distribution in both solid and passing fluid. Heat transfer analysis can be performed without any need to know the magnitude of the convective heat transfer coefficient.

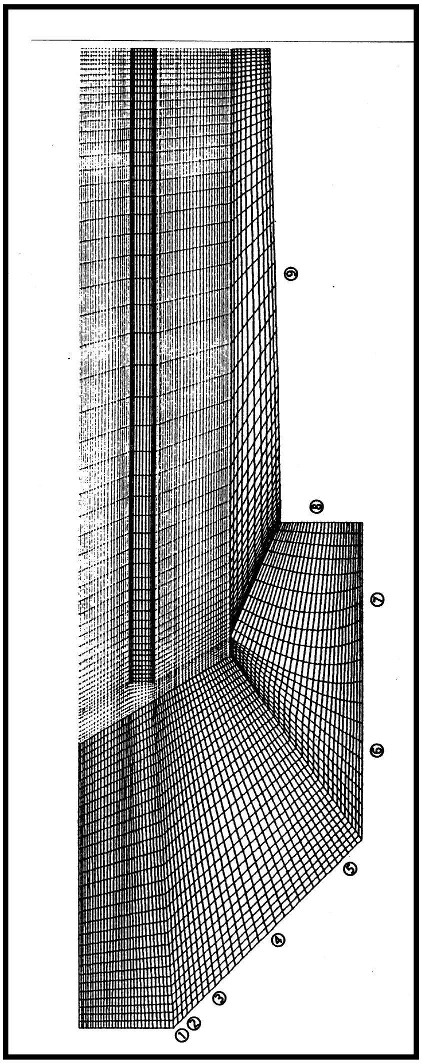

Fig. 3 — Finite element model.

Problem Definition

In the electric resistance spot welding process shown in Fig. 1, electrodes ① and ⑦ press against workpieces ③ and ⑤. A current is then passed through these components. Because of the electrical contact resistance, heat will be generated at electrode/workpiece interfaces ② and ⑥ and faying surface ④. The heat at the faying face melts the workpieces to form a nugget, ④. To prevent melting at the electrode/workpiece interface, water is circulated in the cooling chamber of the electrodes — Fig. 1. For a reduction of the problem size in this investigation, only one electrode was considered. This approach requires knowledge of the power input (determined experimentally) at the electrode/workpiece interface.

Both the ambient air and initial water temperatures were assumed to be 20°C (68°F). If the water does not boil, the physical properties can be assumed to be temperature independent. A complete conjugate heat transfer solution can be performed in two separate steps: 1) a steady-state mechanical solution assuming an imposed coolant flow rate and pressure at the inlet of the water pipe, and 2) a transient thermal solution. This approach — uncoupling the mechanical and the thermal solutions, using the assumption of temperature-independent material properties — substantially reduces the computational time. The welding cycle, *i.e.*, the time to make one spot weld that encompasses several cycles of alternating current, was taken as the duration of the transient solution time.

Table 1 — Weld Cap Geometric Parameters

Parameters	Values
AN	30°
CL	22.0 mm
CR	4.8 mm
HH	6.0 mm
HS	10.0 mm
HW	6.0 mm
MN	0.6 mm
SB	6.4 mm
SH	15.0 mm
ST	6.0 mm
TD	9.0 mm
TI	1.6 mm
TO	2.4 mm
TW	3.0 mm

Table 2 — Material Properties

Parameters	Electrode/ Tube	Water
Density (kg/m^3)	8800	998.3
Viscosity (kg/m-s)	—	1.0E-3
Conductivity (W/m-K)	322	0.5996
Specific Heat (J/kg-K)	390	4182

Table 3 — Effect of Convective Heat Transfer Coefficient (h) on Maximum Tip Surface Temperatures

Power (kW)	h (W/m^2-K)	Temperature (K)
1.818	0	1213
1.818	5	1213
1.818	25	1211

Modeling Discussion

The truncated cone weld cap, a typical production electrode cap, was chosen for this study. A half-section is depicted in Fig. 2 and Table 1 tabulates the corresponding dimensions. For purposes

Table 4 — **Estimated Convective and Radiant Heat Losses at Steady State**

Surface Number	Temperature (K)	Length (mm)	Radius (mm)	Area (mm^2)	Convection Heat Loss (W)	Radiation Heat Loss (W)
1	1018	0.35	3.12	6.86	0.12	0.41
2	957	0.69	3.47	15.04	0.25	0.71
3	855	0.87	4.16	22.74	0.32	0.68
4	651	4.85	6.24	190.15	1.70	1.86
5	549	1.73	8.67	94.24	0.60	0.45
6	549	5.20	9.19	300.26	1.92	1.42
7	446	5.03	9.19	290.45	1.11	0.53
8	446	2.60	7.80	127.42	0.49	0.23
9	344	14.21	6.41	572.31	0.73	0.22
Total					**7.25**	**6.51**

Note: For locations of surfaces in the cap, refer to Fig. 2.

of identification, the end part of the cap marked "TW" in Fig. 2 is referred to as the tip. The shaded region represents the electrode tip body and water tube. The water tube has inner (TI) and outer (TO) radii. The water passage in the cooling chamber has an outer radius of CR and a total length of CL. MN represents the clearance between the water tube and conical base of the cooling chamber. Other designations are self-explanatory. Water tubes in production use have a beveled end; however, by assuming a squared-off end for the water tube as shown in Fig. 2, a 2-D rather than 3-D axisymmetrical model can be used to further shorten the computational time.

Using the geometry described in Fig. 2, an axisymmetric parametric model was generated with *ANSYS Parametric Design Language* (Ref. 9). The model was then "map-meshed" with *FLOTRAN/ ANSYS FLUID141* quadrilateral elements — Fig. 3. Note the fine mesh near the water/electrode interfaces and at the exterior surface of the electrode, where high-temperature gradients are expected.

The temperature independent material properties of the fluid elements (water in the cooling chamber) and the solid (electrode and water tube) are given in Table 2.

Two types of boundary conditions were applied to the finite element model as follows:

1) *Mechanical or flow boundary conditions* — the water flow rate into the water tube and the water pressure in the cooling chamber. Various flow rates ranging from 1.7 L/min (0.4 gal/min) to 7.3 L/min (1.9 gal/min) were used for previous experimental investigations (Refs. 3, 4). Although actual production flow rates were not available at the time of this analysis, a rate of 3.79 L/min (1.00 gal/min), which is believed to be typical of the flow rate employed in practice, was used for this study.

2) *Thermal boundary conditions* — the free convection and radiation from the exterior face of the electrode and power input to the tip.

Values of the convective heat transfer coefficients in free air varied from 5 to 25 W/m^2-K (Ref. 6), with a zero value simulating a completely insulated condition. Table 3 shows the effect of the magnitude of the heat transfer coefficient on the maximum tip surface temperature. These values were calculated using steady-state thermal analysis, ignoring radiation. It appears that convection in free air is not important; therefore, unless otherwise noted, convection in free air will not be considered further.

The convective heat loss from the exterior surface can be found by Newton's Law (Ref. 6) of cooling,

$$Q_i = hA_i\,(T_i - T_o)$$

where h is the convective heat transfer coefficient. (For free convection in air, h has a maximum value of 25 W/m^2-K as mentioned above.) Q_i denotes the heat loss on surface i with area A_i, T_i is the temperature on surface A_i and T_o is the ambient temperature. With an ambient temperature of 200°C (392°F) and T_i obtained from the temperature distribution in the electrode, a maximum total convective heat loss from the weld cap can be estimated. Values for various surfaces of the cap are shown in Table 4. The total heat loss was found to be 7.25 W, which would cause a tip surface temperature change of less than ~2°C (~35.6°F).

The net radiant heat exchange of an ideal black body from surface i and its surroundings, with an absolute temperature of T_o, is given by the Stefan-Boltzmann (Ref. 6) equation:

$$E_i = \sigma\varepsilon A_i\,[T_i^4 - T_o^4]$$
$$= 5.67^*[(T_i/100)^4 - (T_o/100)^4].$$

In this equation, T_i is the absolute temperature of body surface i, σ is a constant with a value of $5.67^* 10^{-8}$ W/m^2-K, and ε is the emissivity. For an ideal black

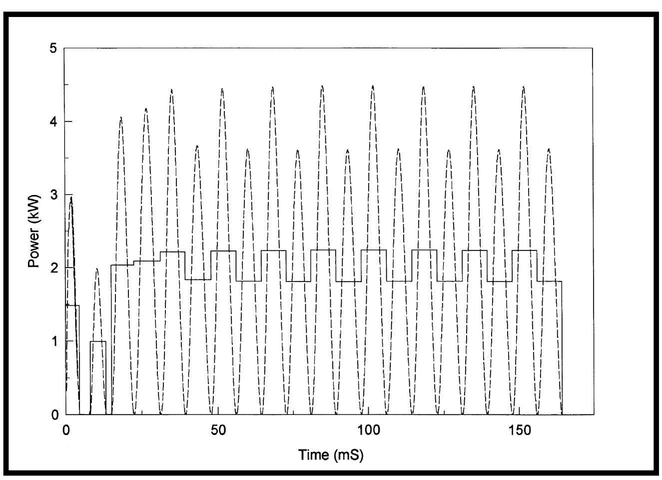

Fig. 4 — Experimental power input (dashed line) and analytic power input (solid line).

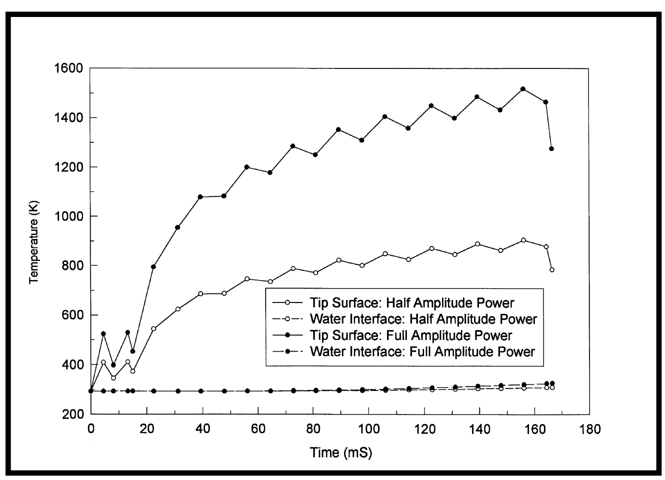

Fig. 5 — Temperature histories of tip working surface and water interface for two power input levels.

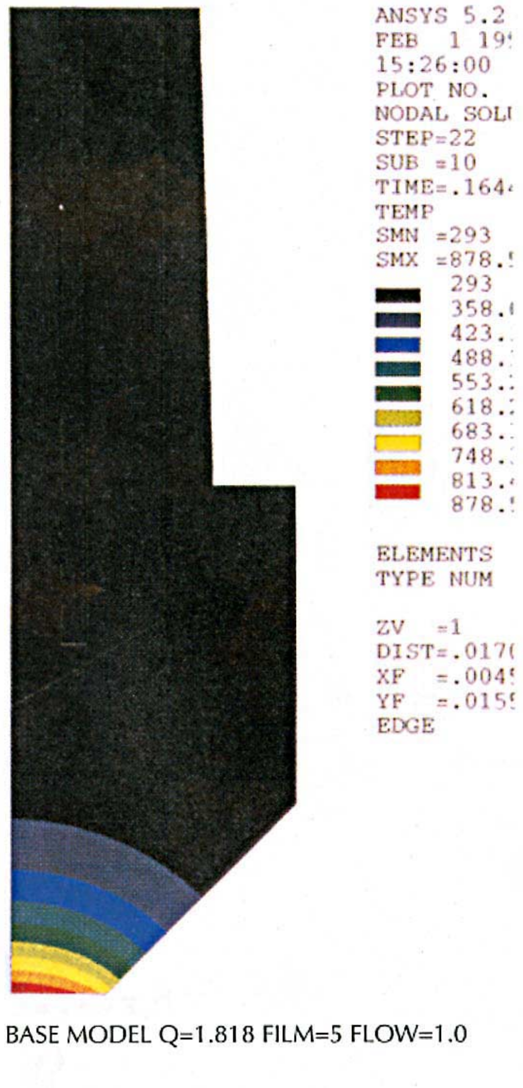

Fig. 6 — Maximum transient temperature distribution in electrode.

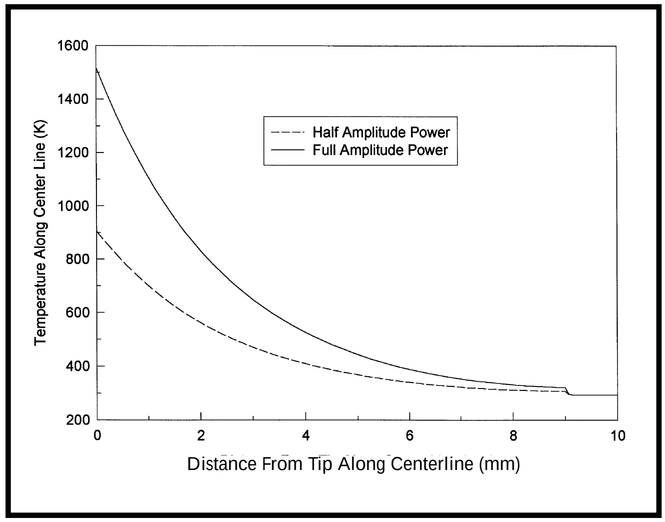

Fig. 7 — Temperature distribution along centerline of electrode cap at end of weld cycle for two power input levels.

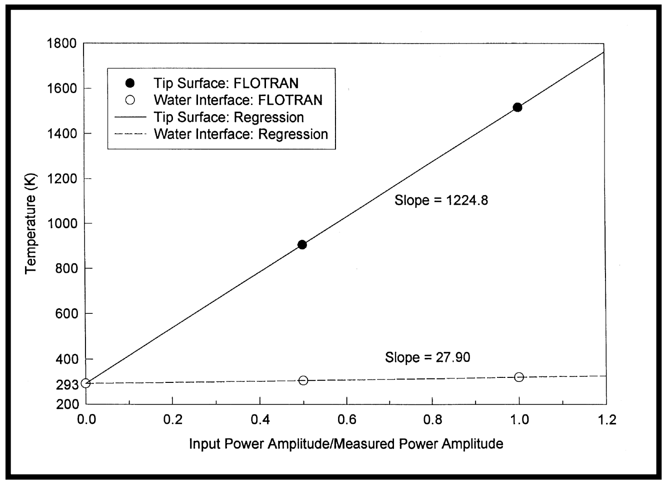

Fig. 8 — Maximum transient temperature vs. power amplitude ratio.

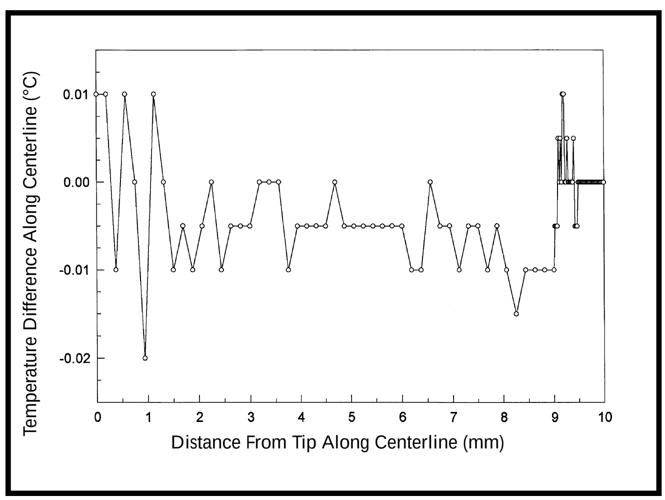

Fig. 9 — Temperature difference between FLOTRAN and linear regression results.

body, ε has a value of 1.0. Estimates of the maximum radiant heat loss from the weld cap are shown in Table 4. The radiant heat loss is even less than the convective heat loss. (Since the maximum convective heat loss contributed to a temperature change of <2°C (<35.6°F), the radiant heat loss was not considered in this analysis.)

This study made use of experimentally determined values for power dissipation at the electrode/workpiece interface in spot welding of aluminum alloys. A typical power dissipation curve (obtained during spot welding an aluminum alloy with a current of 21 kA RMS for 10 cycles) is shown in Fig. 4 (Ref. 10). The total welding cycle time was 0.165 s. The power dissipation estimation involved measurements of both a voltage drop, V, across the interface and a current, I. Ohm's Law, V = IR, yields the contact resistance, R. The power dissipation, W, can then be calculated from the corresponding current profile, I, and the resistance change, R, using the equation $W = I^2R$. For one welding cycle, the total energy derived from the area under the curve was ~300 J and the average power was ~1820 W. If the welding test consisted of one welding (heating) cycle and one cooling cycle, each with an equal time duration, the average power would have been ~910 W. To accentuate the temperature difference, the former power value was used to estimate the maximum convective and radiant heat loss as shown in Table 4.

The computational fluid dynamics software *FLOTRAN* does not permit the use of a ramped power waveform for input. While a sinusoidal power input could have been approximated by a step waveform composed of small steps, this would have made the computational time extremely long. To simplify the calculation, the sinusoidal power input depicted in Fig. 4 was replaced by a step power input, as shown by the solid curve in Fig. 5. For each half-cycle of alternating current (AC), the amplitude of the stepped power was set equal to one half of the maximum amplitude of the corresponding test power for that particular ac cycle period. Thus, for each AC cycle, the energy of the stepped power was approximately equal to that of the corresponding measured power. There were 23 load steps for the transient simulation. For the purposes of subsequent discussion, this power input will be termed "Half Amplitude Power." An additional simulation was performed using a power input twice as large. This latter simulation will be termed "Full Amplitude Power."

Results of Simulations

The temperature changes during the weld cycle at two locations along the line of axisymmetry of the weld cap are shown in Fig. 5. The maximum tip surface temperature for the Half Amplitude Power simulation, 905 K, occurred at the first half of the last AC cycle. The temperature at the cap/water interface, however, increased very slowly, and was only 309 K at the end of the heating cycle. The maximum transient temperature distribution for this current cycle is plotted in Fig. 6.

Experimental evidence (Ref. 10) indicated there were traces of melting of the aluminum workpiece at the tip contact area. Since aluminum alloys typically show incipient melting at temperatures of ~900 K, the tip surface temperature in this simulation was quite accurately predicted. Discrepancies may be attributed to the slight underestimation of the stepped power input and the fact that the model did not include the heat contribution from the faying surface and Joule heating.

At the end of the weld cycle, the maximum tip surface temperature increased from 905 to 1518 K by doubling the input

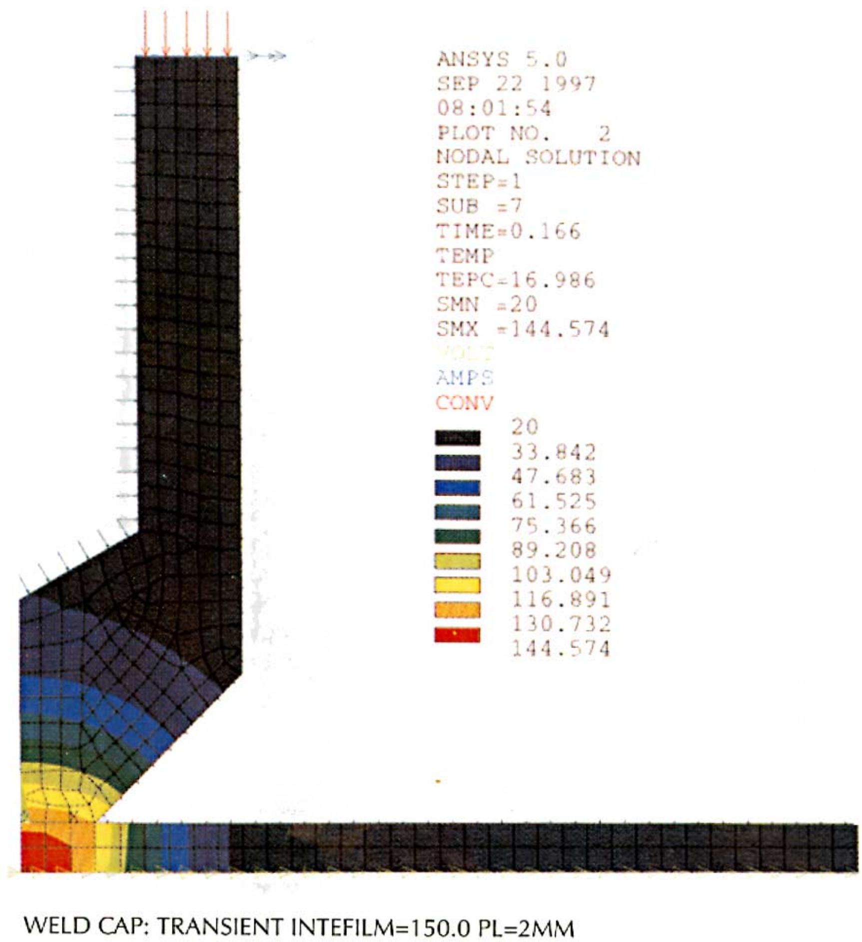

Fig. 10 — Finite element model and temperature distribution for bulk resistive heating of weld cap.

power amplitude ratio from 0.5 to 1.0 — Fig. 7. However, the water temperature showed only a small increase in temperature to 330 K from that determined previously. Temperature profiles along the axis of the cap at the end of the weld cycle for both power simulations are shown in Fig. 8. The temperature gradients near the tip surface and also in the cooling water near the cap/water interface (9.0 mm from the tip surface) were large.

A linear regres-

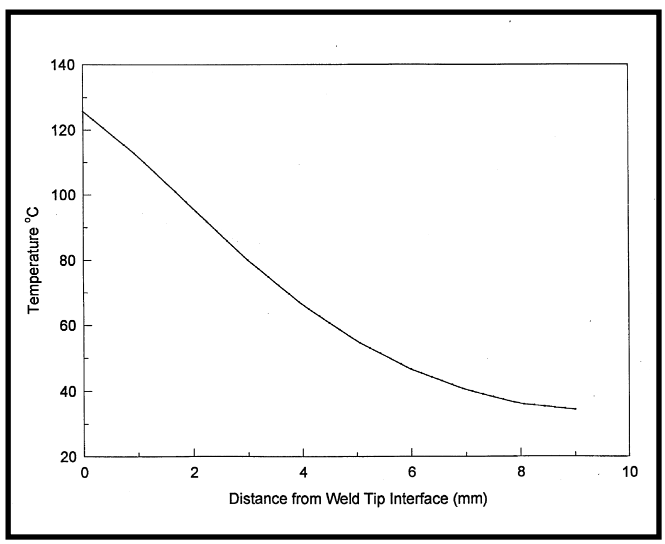

sion was performed on the maximum tip surface and water interface temperatures attained at the end of the weld cycle. Figure 8 shows that the maximum tip temperature varies linearly with the power amplitude ratio. It is notable that this linear relationship also held at other locations along the axis of axisymmetry. Temperature deviations between the *FLOTRAN* and linear regression results are small for the half amplitude power input, as shown in Fig. 9. The linear relation implies that this is a conduction-dominant thermal problem, a conclusion supported by the insignificant convection and radiation losses described previously.

Other parametric studies were also performed, including changing the flow rate from 3.79 to 2.24 L/min and changing the cap depth — TD in Fig. 2 — from 9.00 to 6.35 mm. For the same power ratio, the differences in maximum temperature caused by these changes were insignificant, which is typical for components with a slow thermal response but a fast heating rate.

One limitation of the model used in this analysis lies in the assumption of complete contact at the electrode cap/workpiece interface. In reality, because of irregular surface contours of each surface, actual physical contact is initially made over a limited number of individual contact points. Consequently, very high, but extremely local, temperatures will be reached (Ref. 11) before any significant temperature increase occurs in the main bulk of the cap. This aspect of the model is discussed below.

Resistive Heating of the Weld Cap

Results of the previous analysis indicate that the water temperature is not appreciably raised by one welding cycle of heat input, although the working surface of the electrode weld tip reaches temperatures sufficient to melt aluminum. While water temperatures in the vicinity of the fill tube were not measured directly (generally only the exit water temperature was monitored at a point remote from the weld cap interior), scaling on the interior surface of the weld cap was taken as evidence that water can boil locally during the welding operation (Ref. 12). Joule heating due to the bulk resistance of the electrode could contribute to this effect. To calculate the transient Joule heating, a second, classical heat analysis was performed using typical values for the heat transfer coefficient for the thermal boundary condition and the same current input of 10 cycles, 21 kA RMS used for the conjugate heat transfer analysis. For comparison, two values for the heat transfer coefficient were taken — 150 and 15,000 W/m^2-K (Ref. 6).

Figure 10 shows the model, including the resistive heating from the workpiece, as well as heat loss from the workpiece surface, for the case with the lowest heat transfer coefficient. The temperature contours are indicated and Fig. 11 shows the temperature profile along the centerline axis of the weld cap, from the weld tip interface with the workpiece to the water chamber. The maximum temperature reached at the water/electrode interface by the end of the weld cycle is ~35°C (~95°F), and the calculated maximum temperature at the same position was only slightly lower for the case with the highest heat transfer coefficient.

Although these two heating sources separately do not cause the water temperature to increase to the boiling point of water, in combination it is seen that water temperatures in excess of 100°C (212°F) may be attained. The maximum water temperature caused by the heat generated at the weld tip/workpiece interface is ~70°C (~158°F) combined with the temperature increase caused by current flow in the electrode tip body, ~35°C (~95°F) — Fig. 5.

The observation of water boiling does place a limitation on one of the assumptions used in the analysis, *i.e.*, there was no change of state for the coolant. However, since water boiling was predicted to occur in only a small region, the assumption appears to be plausible. The results highlight the difficulty faced when spot welding low-melting-point-temperature metals such as aluminum, *i.e.*, that the electrode tip working surface rapidly reaches temperatures of the same magnitude as the melting point and that contamination of the tip by alloying will quickly occur.

Conclusions

A parametric model that uses conjugate heat analysis and does not require heat transfer coefficients was developed to predict the transient thermal behavior of spot welding electrodes. The analysis indicated that convective and radiant heat losses were not important. Maximum tip surface temperatures of the same magnitude as the melting point of aluminum alloys were calculated. The rapid temperature development at the working surface of the electrode highlights the difficulties to be expected in designing electrode tips for spot welding metals with low melting points, since tip surface temperatures approaching the melting point of the material being spot welded are rapidly attained. The water temperature increased ~70°C (~158°F) due to the interface resistance heating and ~35°C due to the bulk resistance heating in one weld cycle. The bulk resistance heating increased the cap tip temperature by ~127°C (~260.6°F).

A simple linear relationship between the temperature and the input power amplitude ratio was found, indicating a conduction dominant heat transfer problem. No significant temperature changes were found for a decrease of water flow rate from 3.79 to 2.24 L/min, or a decrease of the cap depth from 9.00 to 6.35 mm. This lack of change may be attributed to a slow thermal response of the electrode for a fast heating rate.

References

1. Hensel, F. R., Larsen, E. I., and Holt, E. F. 1941. Thermal gradients in spot welding electrodes. *Welding Journal* 20(12).

2. Hess, W. F., Wyant, R. A., Stabler, O. E., and Winsor, F. J. 1943. A study of the application of refrigeration to the cooling of spot-welding electrodes. *Welding Journal* 22(11).

3. Browne, D. J., Chandler, H. W., Evans, J. T., and Wen, J. 1995. Computer simulation of resistance spot welding in aluminum: Part I. *Welding Journal* 74(10): 339-s to 344-s.

4. Browne, D., Newton, C., and Keay, B. 1996. Aluminum and steel resistance spot welding: Modelling the differences. *Advanced Technologies & Processes, IBEC '96*, pp. 50–57.

5. Ikeda, R., Yasuda, K., Hashiguchi, K., Okita, T., and Yahaba, T. 1995. Effect of electrode configuration on electrode life in resistance spot welding of galvannealed steel and aluminum alloy for car body sheets. *Advanced Technologies & Processes, IBEC '95*, pp. 144–151.

6. Chapman, A. J. 1987. *Fundamentals of Heat Transfer*. Macmillan, N.Y.

7. Keung, K. S. 1992. Conjugate heat transfer and stress analysis of the 1.91 CFI engine production exhaust valve. *SRL Technical Report No. SR-92-126*.

8. *FLOTRAN*. Compuflo Inc., Charlottesville, Va.

9. *ANSYS User's Manual for Rev. 5.1*, 1994.

10. Thornton, P. H., Krause, A. R., and Davies, R. G. 1995. Spot weld brazing of aluminum alloys. *Proc. Int. Symp. Met. Adv. Light Metals Industries*, CIM, Vancouver, B.C., pp. 217–228.

11. Thornton, P. H., Krause, A. R., and Davies, R. G. 1997. Contact resistance of aluminum. *Welding Journal* 76(8): 331-s to 341-s.

12. Boomer, D. R. 1997. Alcan International Limited, private communication.